Optical studies of spray development in a quiescent chamber and in a direct-injection spark-ignition engine

P.G. Aleiferis, J. Serras-Pereira and Z. van Romunde
Department of Mechanical Engineering, University College London, UK.

D. Richardson and S. Wallace
Jaguar Advanced Powertrain Engineering, Coventry, UK.

R.F. Cracknell and H.L. Walmsley
Shell Global Solutions (UK), Ltd., Chester, UK.

SYNOPSIS

The effects of fuel type and in-cylinder flow on spray formation from a multi-hole injector were studied by high-speed imaging techniques in a quiescent injection chamber and in a single-cylinder Direct-Injection Spark-Ignition (DISI) engine. To examine the effect of fuel volatility on spray formation, the injector was heated from 20 °C to 120 °C in the chamber for *iso*-octane and gasoline. The injection chamber was operated at 0.5 and 1.0 bar to mimic in-cylinder pressures for early injection strategies. Droplet sizing was also employed in the chamber using Phase Doppler Anemometry (PDA). Fuel-type and temperature effects were studied in-cylinder by operating the engine at 20 °C and 90 °C head temperature at 1500 RPM. For both sets of experiments, the study was carried out for two orthogonal views, relating to the tumble and swirl planes of in-cylinder flow motion. Spray formation was observed to be different for the two fuels, especially at high injector temperatures. Wetted footprint spray areas were calculated for both experimental setups.

1 INTRODUCTION

Experimental investigations of spray development are crucial for effective optimisation of different engine combustion systems. However, many investigations into this subject are carried out using single-component fuels due to ease of handling and known, consistent properties (1–4). The ‘success’ of different combustion systems in practice however, is dependent on real-world, multi-component gasoline behaviour. To address this issue, recent work by the current authors has examined the effects of different fuel properties on multi-hole injector spray development, considering a variety of single-component and multi-component fuels in a quiescent chamber (5, 6). In addition, the authors have examined the mixture preparation and combustion in an optical engine using a multi-hole injector for different injection timings with single and split-injection strategies (7). In this paper, the spray development in the quiescent chamber is directly compared to that in the engine to de-couple the effects of in-cylinder flow on spray development through both observation and quantitative comparison of the projected spray areas as viewed from the engine piston crown and a replicated view in the chamber. Spray droplet sizes are also presented, as measured 25 mm below the injector tip for a range of gas pressures and injector temperatures.

2 EXPERIMENTAL SETUP

2.1 Injection system

For both the chamber and engine work the fuel injection system comprised of a pneumatic pump which provided a fuel pressure of 150 bar. The injector used is a prototype with a 6-hole nozzle designed for vertical close spacing arrangement with the centrally located spark plug in the engine. The nozzle essentially accommodates two groups of three holes producing the spray pattern illustrated in Figure 1, where plumes 1 and 6 pass around the spark plug. Due to confidentiality agreements no further details regarding the injector manufacturer or the operating mechanism can be given. However, further details of the fuel supply and injection system, including driver and associated delays, have been quantified and presented in (5).

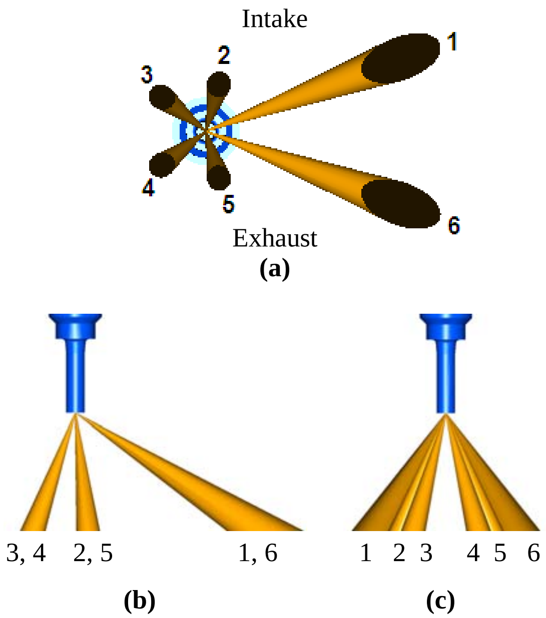

Figure 1. Injector configuration and orientation of spray plumes.

2.2 Fuel properties

The fuels used in this study were *iso*-octane and a pump-grade gasoline that has been commercially available in continental Europe. Figure 2 illustrates the distillation curves for the fuels and highlights the single boiling point of *iso*-octane at ~99 °C.

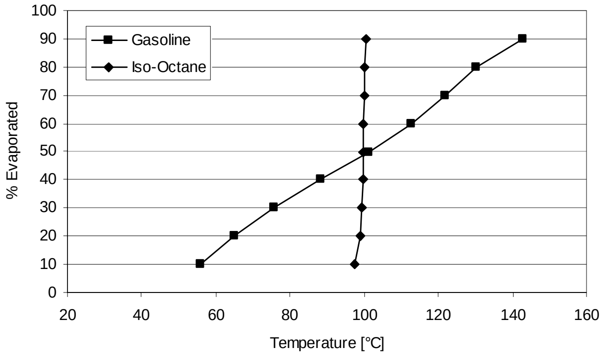

Figure 2. Fuel distillation curves.

2.3 Optical pressure chamber

Imaging and drop sizing of the fuel sprays was carried out in a pressure chamber that has been designed with an octagonal geometry for application of simultaneous optical diagnostic techniques, as shown in Figure 3(a). In addition to side windows, the chamber was fitted with a quartz window in its base to replicate the piston crown view of the optical engine. The injector was mounted at the top of the chamber at an angle of 19° to allow optimised imaging of all three injector spray plume pairs, as will be shown in the results section. Further details pertaining to the chamber and associated instrumentation can be found in (5, 6). The injector body was heated by an Omega MB1 150W band heater and temperature control feedback was provided via a K-type thermocouple located as near to the injector tip as physically possible with closed loop control. As such, the assumption has been made that given a heat soak time of at least half an hour, the fuel temperature inside the injector nozzle had risen to that of the injector body. The spray was either back-lit or side-lit by a Multiblitz Variolite 500 photographic flashgun and was imaged on 640×480 pixel-resolution frames using a high-speed CMOS camera (Photron APX-RS) set at a frame rate of 9 kHz, corresponding to 1° CA between frames for an engine running at 1500 RPM. Each imaging test batch consisted of 100 spray events per condition. Droplet sizing was carried out using a TSI Phase Doppler Anemometry (PDA) system consisting of a Coherent Innova 70C Argon-Ion laser coupled to a TSI beam splitter and Bragg cell. Both the transmitter and receiver had an optical focal length of 250mm. The PDA technique is well documented in the literature and numerous authors have examined the influence of both hardware and software settings on the measured values (8–10), so no further details will be provided here. The droplet size measurements were taken 25 mm downstream from the injector tip along the chamber central axis in the central region of plume 2. Due to the complex geometry of the nozzles, a plate was placed near the injector tip which allowed the unobstructed passage of plume 2 for all conditions, whilst deflecting the other plumes away from the PDA measurement volume. 200 injections were measured at each test point. Injector and instrumentation triggering was provided by an AVL 427 Engine Timing Unit. The chamber was purged after every 20 injections of 2 ms duration each for both imaging and droplet sizing techniques to prevent the build up of fuel vapour and obscuration of measurements.

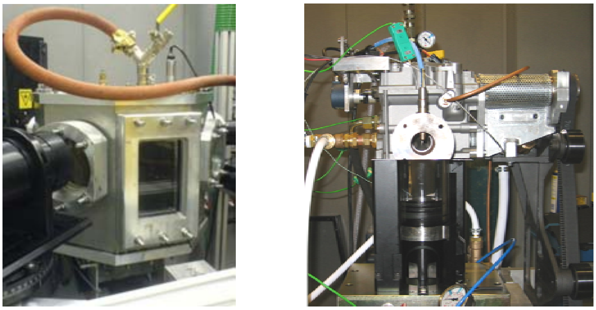
(a) **(b)**

Figure 3. Optical pressure chamber and optical single-cylinder engine.

2.4 Optical single-cylinder engine

The single-cylinder engine used for this work is based on a modular Ford (US) design using a prototype Jaguar DISI engine head, as shown in Figure 3(b). The engine has 2 intake and 2 exhaust valves, a bore of 89 mm and a stroke of 90 mm. A number of optical configurations are possible depending on the level of in-cylinder access necessary. In-cylinder pressure was measured with a Kistler 6041 water-cooled piezo-electric pressure transducer. A piezo-resistive absolute pressure transducer was installed in the inlet plenum to set the engine load by adjusting the throttle. Further details on the engine and test bed can be found in (7). The engine was motored at 1500 RPM under part-load (0.5 bar intake pressure) and at full-load (1 bar intake pressure) conditions. Injection was set early in the intake stroke to promote mixing and evaporation during the intake and compression strokes. In total 100 cycles were recorded for every condition. Images were recorded with the Photron APX-RS CMOS camera at a frame rate of 9 kHz through the piston crown (640×480 pixel resolution), to give a temporal resolution of 1° CA at 1500 RPM, and at 5 kHz for the images through the quartz liner (512×1024 pixels), giving 1.8° CA resolution at 1500 RPM. Imaging was performed with illumination from a high-repetition rate Nd:YLF laser, using either flood or laser-sheet lighting. Laser-sheet imaging was performed on two orthogonal planes. A vertical plane, termed ‘tumble plane’, ‘sliced’ the injector tip through the centre thereby allowing mainly the imaging of spray plumes 2 and 5, see Figure 1(a, c). A horizontal plane allowed imaging of the ‘footprint’ of all the spray plumes as these penetrated down into the cylinder bore at a vertical location 1 mm above the head gasket (*i.e.* 1 mm into the pent-roof). This plane will be referred to as the ‘head gasket plane’. The influence of temperature was observed by controlling the engine coolant from 20–90 °C.

3 RESULTS AND DISCUSSION

Instantaneous images of typical sprays taken for gasoline and *iso*-octane in the quiescent chamber at 0.5 bar are presented in Figure 4 for two timings After the Start Of Injection (ASOI, time interval after the start of the trigger pulse sent to injector driver) and for two fuel temperatures (20 °C and 120 °C). As mentioned earlier, the injector for these experiments was mounted at an angle of 19° and so reference should be made to the schematic diagram shown at the top of this figure, defining the imaged views termed 'side', 'angle', 'end' and 'base'. The effect of increasing the temperature at this low pressure condition is clearly illustrated in the images of Figure 4, namely the contraction and combination of the closely spaced plumes (termed spray 'collapse') for the multi-component gasoline. *Iso*-octane can be observed not to exhibit the same extent of 'collapse' at the same condition.

The spray was also imaged in-cylinder through the piston crown with the engine not running (*i.e.* 'static') so that a baseline image of the spray at atmospheric conditions was available for comparison with the injector rig and the motoring engine. The top row in Figure 5 shows the spray development for gasoline at 'static' engine conditions on the head gasket plane. This is similar in pattern to that observed in the chamber for the same 'ambient' conditions. The line of symmetry between the top and bottom pair of nozzles is clearly seen, as expected from the design of the injector that has been presented schematically in Figure 1. In contrast, the second row of images in Figure 5 shows the spray development with the engine motored at 0.5 bar intake pressure and with an injection timing of 80° CA After intake Top Dead Centre (ATDC). The injection duration was set to 0.78 ms (~7° CA), corresponding to stoichiometric conditions for a firing engine at that load. The effect of flow on spray development is evident as the symmetry of the spray plumes is destroyed and, in particular, spray plumes 1 and 6 are deflected towards the exhaust side by the intake flow. Spray deformation and break-up is also demonstrated by the increased area of light scattering around the spray cores relative to the static condition. Although there are reports in the literature suggesting that the engine intake flow has a relatively small effect on the in-cylinder spray development for pressure-swirl atomisers (11, 12), such interactions are highly sensitive to both engine operating conditions and engine/injection system used. In the current study of a multi-hole injector with a complex layout, the levels of interaction between the spray and air motion will be different for each plume and will be governed by the magnitude, duration and incident angle of the flow over the intake valves that forms an intense 'valve jet'. The intake flow has been characterised by Particle Image Velocimetry (PIV) in an engine of identical configuration (13) and it has been shown that the valve jet reaches its peak magnitude at ~80°–90° CA ATDC which coincides with the injection event in the current study. Maintaining the same injection timing and increasing the engine load (1 bar intake pressure) has an even more dramatic effect on spray formation during and after the injection event, as shown in the third row of Figure 5. For comparison with the part-load operation, the injection duration for stoichiometric firing of the engine at full-load was 1.6 ms (~14.5° CA).

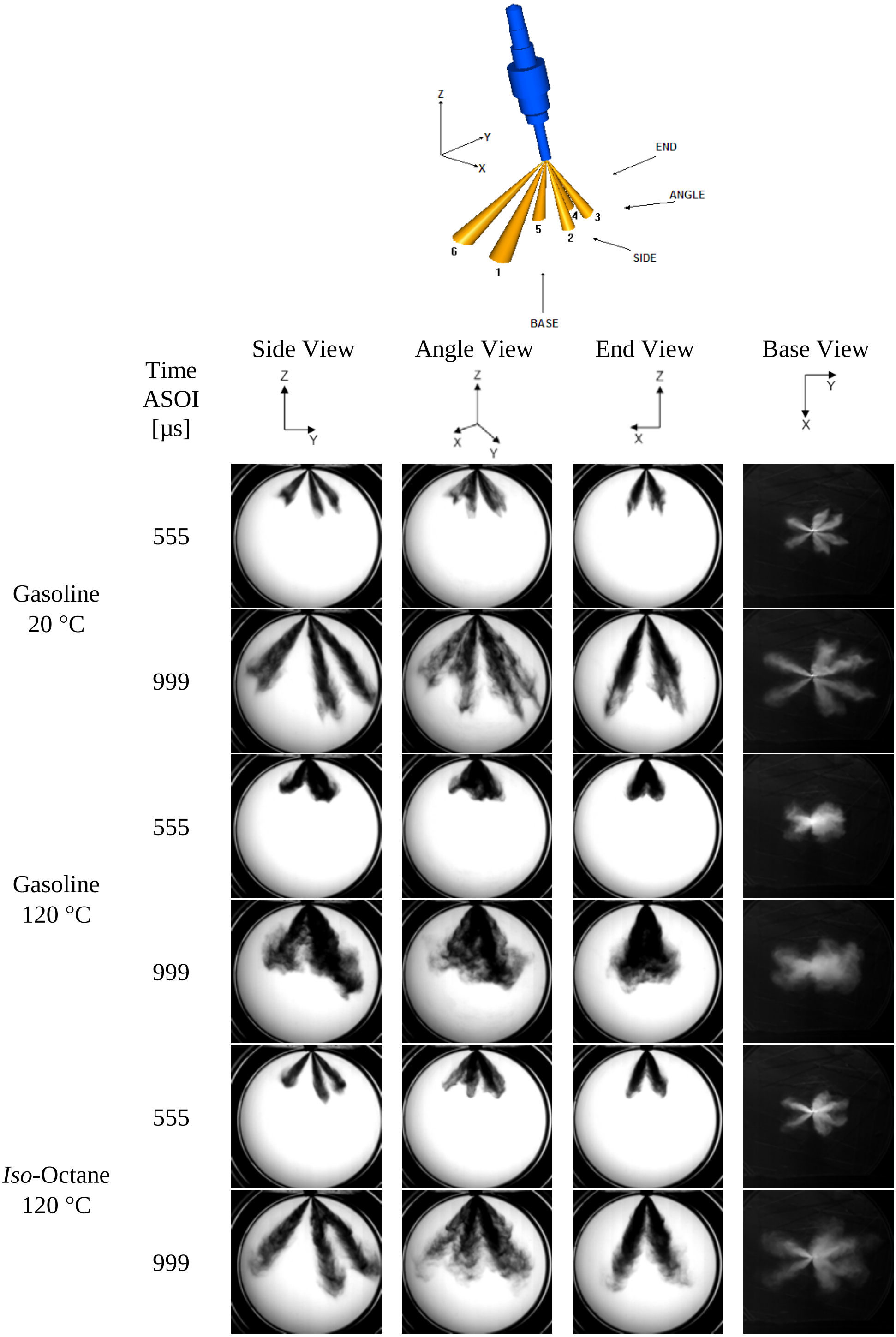

Figure 4. Spray development in the pressure chamber (gasoline and *iso*-octane).

The in-cylinder spray development for the part-load operating condition (0.5 bar intake pressure) is shown in Figure 6 for gasoline fuel and for single representative cycles at 20° C and 90 °C engine head temperature (SOI 80 °CA ATDC). The left column shows the spray formation on the tumble plane using laser-sheet imaging, the central column shows the spray formation on the head gasket plane and the right column shows the spray formation through the piston crown using flood illumination for direct comparison with the chamber 'base' view spray images. Laser-sheet imaging allowed clearer determination of penetration variability and spray plume targeting on planes similar to those used for the PIV measurements in (13), whereas global imaging provided insights into the 3-D nature of the air-fuel interactions over the whole injection duration. The effects of engine temperature on spray development are evident in Figure 6 and similar in nature to those presented earlier in the chamber in Figure 4. However, the flow field effects in the engine do alter the spray characteristics. The primary point of note is that in the engine a 'normal' spray formation is observed at low engine head temperatures, Figure 6(a), whilst a 'collapsed' spray is seen at 90 °C engine head temperature, Figure 6(b). In the chamber the spray is only partially collapsed at 90 °C, hence comparison at high temperatures is best made between the chamber sprays at 120 °C injector temperature and the in-cylinder sprays at 90 °C engine head temperature.

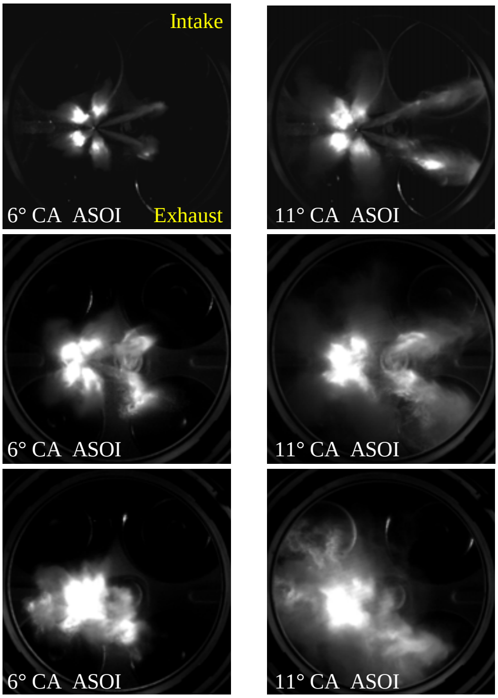

Figure 5. In-cylinder gasoline spray development. Top row: static engine; Middle row: motored engine 0.5 bar intake pressure; Bottom row: motored engine 1.0 bar intake pressure (engine head 20 °C).

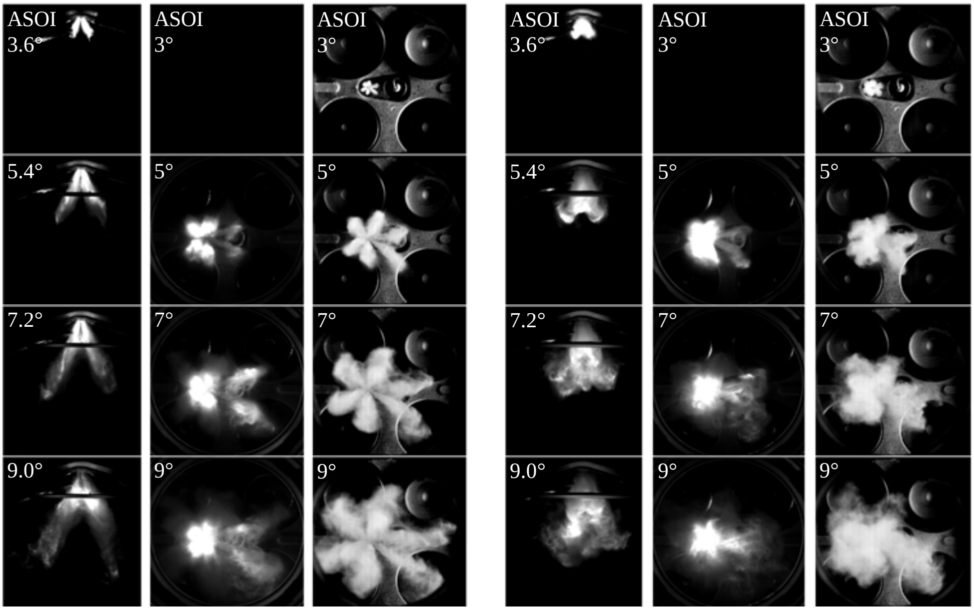

(a) **(b)**

Figure 6. In-cylinder gasoline spray development. Engine head (a) 20 °C, (b) 90 °C. Left: tumble plane; Centre: head gasket plane; Right: flood imaging.

To illustrate the effect of the in-cylinder air flow on spray formation the spray areas as viewed through the piston crown (*i.e.* the flood-illumination images in Figure 6) are compared to the equivalent spray images in the chamber (*i.e.* the ‘base’ view in Figure 4). Spray images from both experimental set-ups were binarised using appropriate thresholding and these were used to calculate the ‘wetted footprint’ spray area. The spray images acquired in the chamber were corrected for the 19° injector inclination angle. Each calculated area was then normalised by the area of the engine piston crown window that was 65 mm in diameter. Figure 7 shows the normalised areas for 0.5 bar chamber and intake pressures. As can be seen from this graph, the overall trends concerning the differences in spray development for the two fuels are replicated in both the engine and chamber. These observations mirror the comments made earlier when comparing the respective spray images. The air motion effect on the in-cylinder measurements can be observed from the larger areas calculated for the engine sprays due to increased degree of mixing between the air and the liquid fuel. In both engine and chamber, the rate of growth of area is initially larger at collapsed spray conditions and then reduces to below that of the non-collapsed spray pattern. This is probably due to the greater constant radial component of the outwardly growing plumes for the non-collapsed case. In both experimental setups, the spray area viewed for *iso*-octane for all conditions is smaller than gasoline’s, except at 20 °C in the chamber where both fuels show nearly identical calculated spray areas. This difference is thought to be due to the multi-component nature of the evaporation process of the gasoline fuel, in particular the vaporization of the light fractions 'swelling' the spray plumes. After the end of injection in the engine (~1200 µs) the spray area of *iso*-octane reduces at a faster rate in comparison to gasoline.

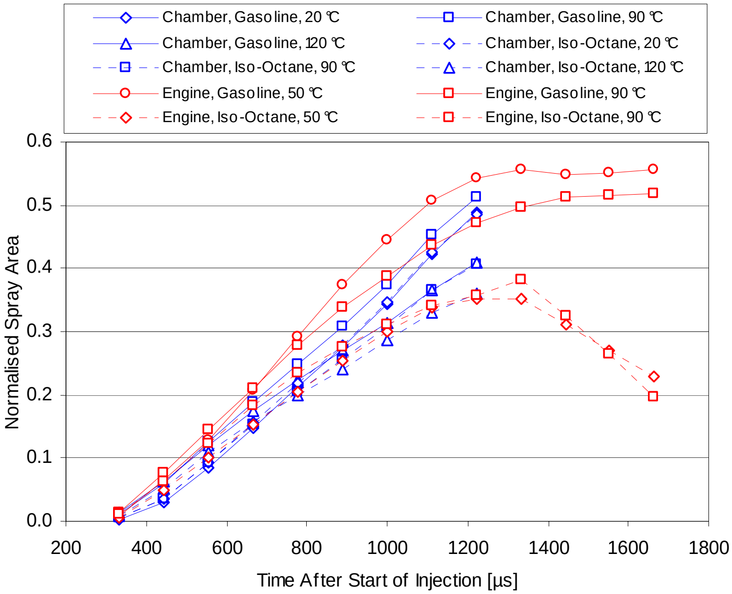

Figure 7. Spray areas through the base chamber view and the piston crown.

In order to investigate further the link between the spray development and atomisation, including the observed differences in calculated spray areas in the chamber and in the engine, droplet sizing was carried out in the chamber for a range of gas pressures and injector temperatures. Figure 8 shows the Sauter Mean Diameter (SMD, $D_{3,2}$) measured 25 mm below the injector tip for plume 2 using gasoline. This shows that droplet sizes reduce with both a decrease in gas pressure (for a given injector temperature) and an increase in injector temperature (for a given gas pressure), ranging from ~17 to 9 µm. Spray images at 777 µs ASOI have been superimposed on the graph to aid interpretation. Initial convergence of the far right plume pair can be observed to occur from the images when the measured SMD falls below ~12 µm. A similar trend between droplet size and onset of collapse was observed to occur in measurements taken for single-component fuels, but not presented here. At the same distance from the injector tip (25 mm) and at a fuel temperature of 90 °C using a "multi-component petroleum product" van der Wege and Hochgreb (14) measured an SMD of approximately 16–19 µm in a square bore engine for an intake pressure of 0.6 bar and an injection pressure of 50 bar, the exact value of the SMD being a function of the radial distance from the injector axis for the pressure swirl injector tested. These droplets are slightly larger than those measured for the multi-hole injector under investigation here; the increased fuel pressure and the alternative form of atomisation utilised would both lend themselves to the production of smaller droplets.

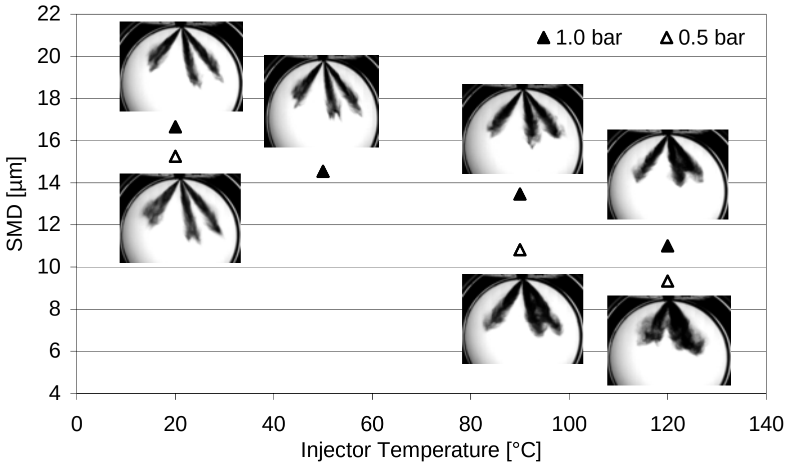

Figure 8. Droplet sizes for gasoline sprays.

4 CONCLUSIONS

Spray development from a multi-hole DISI engine injector was compared in a quiescent chamber and in a single-cylinder optical engine. High-speed imaging and droplet sizing techniques were employed to study the effect of fuel type, injector temperature and in-cylinder pressure. The following conclusions can be drawn:

- The development of sprays produced using *iso*-octane and pump-grade gasoline fuels vary considerably at increased fuel temperature and reduced gas pressure which has implications on the use of *iso*-octane for the diagnostics of injection systems and engines in general.
- Onset of spray collapse was observed for gasoline in the quiescent chamber at conditions of 0.5 bar gas pressure and 120 °C injector temperature. In the engine a similar degree of collapse was observed for 0.5 bar intake pressure and 90 °C engine head temperature.
- The wetted footprint of the fuel spray increases initially for both gasoline and *iso*-octane as injector temperature is raised from 20 °C to 90 ° C in the chamber. Similar observations were made for the in-cylinder spray formation when the engine head temperature was raised from 50 °C to 90 °C.
- Further increase in injector temperature for the quiescent chamber sprays leads to a reduction in wetted footprint as the spray is drawn into the area directly below the injector tip, concentrating along the chamber axis as it ‘collapses’.
- The area of the wetted footprint of the spray is smaller for *iso*-octane than for gasoline due to the single boiling point of *iso*-octane and its uniform propensity to evaporate at any temperature.
- At the onset of spray collapse the SMD of the spray was measured to be below 12 µm.

ACKNOWLEDGEMENTS

Support from the EPSRC (grant GR/S58850/01), Jaguar Cars and Shell Global Solutions is gratefully acknowledged.

REFERENCE LIST

(1) Gavaises, M., Abo-Serie, E. and Acroumanis, C., “Nozzle Hole Film Formation and its Link to Spray Characteristics in Swirl-Pressure Atomisers for Direct-Injection Gasoline Engines”, SAE Paper 2002-01-1136, 2002.

(2) Alexander, P., Begg S., Heikal, M., Li G. and Gold, M., “Airflow and Fuel Spray Interaction in a Gasoline DI Engine”, SAE Paper 2005-01-2104, 2005.

(3) Hayakawa M., Takada S., Yonesige K., Nagaoka M. and Takeda K., “Fuel Spray Simulation of Slit Nozzle Injector for Direct-Injection Gasoline Engine”, SAE Paper 2002-01-1135, 2002.

(4) Mitroglou, M., Nouri, J.M., Yan, Y., Gavaises, M. and Arcoumanis, C., “Spray Structure Generated by Multi-Hole Injectors for Gasoline Direct-Injection Engines”, SAE Paper 2007-01-1417, 2007.

(5) van Romunde, Z. and Aleiferis, P.G., “Effect of Operating Conditions and Fuel Volatility on Development and Variability of Sprays from Gasoline Direct-Injection Multi-Hole Injectors”, Atomization and Sprays, in Press, 2007.

(6) van Romunde, Z., Aleiferis, P.G., Cracknell, R.F. and Walmsley, H.L., “Effect of Fuel Properties on Spray Development from a Multi-Hole DISI Engine Injector”, SAE 2007 Powertrain & Fluid Systems Conference and Exhibition, October 29–31, Chicago, USA, SAE Paper 2007-01-4032, 2007.

(7) Serras-Pereira, J., Aleiferis, P.G., Richardson, D. and Wallace, S., “Mixture Preparation and Combustion Variability in a Spray-Guided DISI Engine”, SAE 2007 Powertrain & Fluid Systems Conference and Exhibition, October 29–31, Chicago, USA, SAE Paper 2007-01-4033, 2007.

(8) Albrecht, H.-E., Borys, M., Damaschke, N. and Tropea, C., “Laser Doppler and Phase Doppler Measurement Techniques”, Springer-Verlag, 2003.

(9) Araneo, L. and Tropea, C. “Improving Phase Doppler Measurements in a Diesel Spray”, SAE Paper 2000-01-2047, 2000.

(10) Wigley, G., Goodwin, M., Pitcher, G. and Blondel, D., “Imaging and PDA Analysis of a GDI Spray in the Near-Nozzle Region”, Experiments in Fluids, Vol. 36, pp. 565–574, 2004.

(11) Kashdan, J.T., Shrimpton, J.S. and Arcoumanis, C., “Dynamic Structure of Direct-Injection Gasoline Engine Sprays: Air Flow and Density Effects”, Atomization and Sprays, Vol. 12, pp. 539–557, 2002.

(12) Davy, M.H., “Effect of Impinging Airflow on the Near Nozzle Characteristics of a Gasoline Spray from a Pressure-Swirl Atomiser”, SAE Paper 2006-01-3343, 2006.

(13) Justham, T., “Cyclic Variability of Engine Intake and In-Cylinder Flows”, PhD Thesis, Loughborough University, UK, in Preparation, 2007.

(14) van der Wege, B.A. and Hochgreb, S., “Effects of Fuel Volatility and Operating Conditions on Fuel Sprays in DISI Engines: (2) PDPA Investigation”, SAE Paper 2000-01-0536, 2000.